UNIVERSITY OF COPENHAGEN
NIELS BOHR INSTITUTE

Bachelor's thesis

Author: Maliha Shfagat Khan

Forbush Decreases and Atmospheric Parameters

Analyses of the possible relationship between sudden drops in galactic Cosmic Ray (GCR) flux, and atmospheric parameters. Analyses are based on re-analysis weather data and medium range weather forecasts.

Supervisor: Eigil Kaas

Submitted on: June 12th 2019

Abstract

This study aims to investigate the short-term drops in galactic cosmic ray (GCR) known as Forbush Decreases (FD) and compare these with the changes in the cloud parameters in order to verify the correlation between clouds and GCR. This study is largely based on a statistical Monte Carlo bootstrap method which is developed to rank FDs in the GCR radiation according to their expected impact on the ionization of the lower atmosphere, this method is developed by Svensmark. et al (2016). The cloud parameter data includes satellite data of cloud fraction (CF) from MODIS satellites and medium-range weather data of the total cloud cover (TCC) the European Centre for Medium-Range Weather Forecasts (ECMWF) which is essential for this study. The analyses are done in two steps: 1) for the period 2000-2007 and 2) for the period 1990-2007. The average signals in the re-forecasts for the periods 2000-2007 and 1990-2007 are both, with high significance, showing that the re-forecasts are following the re-analyses closely. Our conclusion is that FDs doesn't affect the medium range weather forecasts as first thought i.e. our investigation rejects the GCR-clouds link.

Table of contents

ABSTRACT **1**

1. INTRODUCTION **3**

2. FORBUSH DECREASE AND CLOUDS **3**

2.1 Eliminating Space Weather in Atmospheric Models 5

3. DATA **5**

4. METHOD **6**

4.1 Monte-Carlo Bootstrap-based statistics 7

5. RESULTS **9**

6. DISCUSSION AND CONCLUSIONS **12**

REFERENCES **15**

APPENDIX **16**

1. Introduction

The link between cloud formation and galactic cosmic ray (GCR) has been studied in several studies in the past since Nye suggested that GCR may affect the Earth's weather and climate (1959). There has been a great evolution in instrumentation and computations which is now enhancing the ability to make more detailed studies of it. Svensmark and Friis-Christensen published one of the first original investigation on the possible link between solar variability and cloud cover by using long continuous data series obtained by satellite and neutron monitors [11]. According to the hypothesis there is an inverse connection between solar variability and atmospheric parameters via the geomagnetic field, i.e. when more GCRs penetrate the atmosphere more ionized particles are formed in a secondary particle shower, ionized particles add more material to aerosols which in formation phase into cloud condensation nuclei add more and bigger clouds to the atmosphere [10]. This hypothesis has been tested by Svensmark at CERN's CLOUD experiment whose purpose was to detect how ionizing particles from a proton synchrotron affect the aerosol formation from a test vapor. The CLOUD experiment showed that growth rate of aerosols is promoted after being hit by ionized particles. The results are from modelling point of view not entirely equivalent to the real atmosphere, it is uncertain how the promoted growth of aerosol translates to observable changes in the clouds [9]. However, these increased growth rates haven't been possible to obtain for the temperatures similar those in the lower troposphere [7]. In addition, modeling studies of cloud condensation nuclei (CCN) shows that CCN is not sensitive toward changes in ion-production over a solar cycle [7]. In order to validate the significance of this link, this study looks at the sudden drops of GCR by coronal mass ejections (CME) known as Forbush decreases which shall lead to less cloud cover on Earth in the days after the decline. The duration of the decline in cloud cover is short-term only. Depending on how strong the FD is, the clouds regulate themselves back to normal after ~8-13 days. The evolvement of more accurate weather forecasts opens a new opportunity for verifying how big the FD affects the Earth's climate and weather system. The error of ERA-Interim (ERA-I) is used as the key factor for determining this effect. The ERA-I re-forecasts has a lead time of 10 days. The ERA-I re-forecasts are in this study viewed as the 'normal' state of the atmosphere since it is based on atmospheric models which are not aware of space weather conditions such as CMEs. On the other hand, ERA-I re-analyses are induced from numerous observations and it can therefore be affected by multiple different conditions. A more comprehensive description of the terms *ERA-I*, *re-analyses* and *re-forecasts* is written in section 2.1 and 3. This study will largely compare data re-analyses and re-forecasts with the same FDs and method developed by Svensmark, J, [9]. The FDs are ranked due to ionization (strength) and the method used to validate significance is a Monte Carlo bootstrap statistical analysis.

2. Forbush Decrease and Clouds

Coronal Mass Ejections (CMEs) are massive eruptions in the solar atmosphere, and they can have a diameter larger than the sun itself. After this spectacular event occurs, it interacts with the Earth (and other planets) by producing series of impacts on the terrestrial environments and the human

high-tech activities. The CMEs results in hazardous space weather conditions especially nowadays where high-tech activities are more common and still being developed. One of the many impacts resulting from the CMEs are the reduction of galactic cosmic rays (GCRs) into the Earth's atmosphere. The GCRs is of extraterrestrial origin, and they can be divided into two groups known as primary and secondary groups. The GCRs are highly energetic particles which consists mostly of protons (~89%) and helium nucleus (~10%) and some heavier particles (~1%). The primary GCR is charged particles that interacts with the upper atmosphere meanwhile the secondary GCR is interactions in the lower atmosphere due to the constituents from the primary interaction. The individual FDs are typically measured by neutron monitor stations which measures the shock and ejecta during the FD. The neutron measurements are converted into time series of percentage intensity or fluxes. The flux of GCRs in the atmosphere is modulated by both the magnetized solar wind plasma and the geomagnetic field. The deflection of GCRs due to the geomagnetic field depends on the *cut-off rigidity*, R_c, which is the minimum energy or momentum required to penetrate the atmosphere and it depends on latitude coordinate.

If we assume the magnetic field of the Earth is approximately a dipole field, then the cut-off rigidity R_c for vertically incident particles [4]:

$$R_c = \frac{M\mu_0 c}{16\pi RE^2} \cdot (\cos\lambda)^4 \tag{1.1}$$

Where M is the dipole moment, μ_0 the permeability of free space, c the speed of light, RE the radius of the Earth and λ the geomagnetic latitude. Rigidity is measured in voltage (V) and the cut-off rigidity is a measure for the minimum value (of rigidity) required to penetrate the magnetic field of Earth. The geomagnetic field dependency induces a cut-off rigidity which is higher near equator (low latitudes) and lower in the mid- and high-latitudes where more GCR can penetrate the lower atmosphere. In particular, this is caused by the shielding effect of the Earth's magnetic field - the magnetic lines are nearly horizontal at equator and vertical at the magnetic poles. However, equation (1.1) is not used in the calculations in this study.

The GCRs are considered as sources of the ionization in the lower atmosphere where they can affect microphysical phenomena related to the atmosphere. When a major magnetized solar wind plasma is escaped from the sun in an event known as CME it decrements the GCR by up to 1%. These decrements are called Forbush decreases (FD) and they typically last for a couple of days. FD is an "Earth phenomenon". In short, CME act as a screen toward GCR and the resulting reduction in GCR in the atmosphere is known as FD event. The GCRs in combination with CME control the electrical system, which according to the hypothesis control cloud microphysics and radiative transfer within the atmospheric system. It is important to note that the modulations in GCR due to solar variability and the magnetic field of Earth happens on different time scales - if this wasn't the case it could be almost impossible to study the link between solar variability and climate. The Sun alone changes its activity on numerous time scales that vary from 27 days to 11, 22, 80, 106, 212 years, and more [5]. The changes between minima and maxima in total solar irradiance (TSI) during the 11 years is 0.15% [5]. However, these changes are not resulting in the dominating anomalies in the Earth that we are interested in. These cycles don't take into account the eruptional events such as solar flares, wind bursts from coronal mass ejections, and solar wind

bursts from coronal holes, that are hypothesized to have much greater impacts in short- and long-term Earth phenomena. This gives rise to investigate the linkage between FD and the cloud nature.

2.1 Eliminating Space Weather in Atmospheric Models

This study uses both satellite-based data from Moderate Resolution Imaging Spectroradiometer (MODIS) and model-generated data from the European Centre for Medium-Range Weather Forecasts (ECMWF) for re-analysis and re-forecasts for the weather. The re-analysis data from ECMWF is modeled initial states of the atmosphere and the satellite data from MODIS also contributes to the re-analyses. The impacts from GCR on the atmospheric state is analyzed by comparing re-analyses with re-forecasts. By re-analyses we mean past global observations which are assimilated into a stationary data assimilation system and atmospheric model - in our case the Integrated Forecasting System (IFS) from ECMWF. The IFS from ECMWS is a leading data assimilation system where any types of observation instruments i.e. satellite observations, weather stations, buoys, ships etc. are put into a model to give the best initial value (weather situation) at a given time. The IFS model treats all past observations with the same method. The IFS create initial values for a numerical weather prediction (NWP) model - this is the essence of *data assimilation*. The re-forecasts are predictions made forward in time based on re-analyses. A success scenario in our study will be to prove that external sources like Forbush decreases cannot be predicted since they are beyond the scope of the parameters that are included in the equations used for making NWPs. NWP models uses the atmospheric models from meteorology, which includes seven equations: balances for mass, water mass, the three-dimensional momentum and energy, and the ideal gas law. These equations don't account for external forcing and impacts from sources outside the atmosphere. Through the comparisons of re-forecasts with re-analyses and observations we'll be able to verify the radiative forcing in the atmosphere from a Forbush decrease. The comparison between re-analysis and re-forecast allows us to eliminate signals due to weather noise in our variable. Hence, we can track the short-term impacts on the atmosphere due to FD. Clouds will regulate itself after some days due to its own physical processes which is mostly non-weather-related. The clouds' ability of knowing past incidents will be referred as their *memory*. Their memory is related to complex microphysics which is not fully understood yet. The duration of the cloud memory is thought to be less than a week if we consider the average life-time of a cloud condensation nucleus. This is also seen in the results we obtained from applying the Monte Carlo bootstrap statistics – the time-interval between the decline in cloud cover and the time-step where it begins to rise again is about 5-10 days. In our particular data, it makes more sense to set the times of the signal integral of the FD-event t_1 to 4 and t_2 to 10, our time-interval contains 6 days, the signal integral *FS* is presented section 4.1.

3. Data

The dataset includes data from NASA's remote sensing MODIS satellite which measures atmospheric, land and ocean variables with imaging. It is used because FDs are thought to have strong visible impacts on the global cloud cover. The dataset is from the data product named 'MOD08_D3' and the parameter we look at is 'cloud fraction liquid mean (CF)'. The other data

are from ECMWF's ERA-I global atmospheric re-analysis datasets. ERA-I is a product that contains various atmospheric variables that has been measured by an IFS model which is developed at ECMWF. The IFS model used in ERA-I uses measurement from way back in 1979 to present day to create modeled initial states for the atmosphere i.e. re-analyses. The IFS model embraces observations from various instruments unequally distributed over the globe to make interpolations for the entire globe. Re-forecasts uses re-analysis data as initial states and makes predictions for the future in intervals of 12 h and here we use forecasts for time-steps 12h, 24h, 36h, 48h and up to 144h (6 days). ERA-I has a lead time of ten days but we are only using re-forecasts up to six days for research. The parameters we use are 'total cloud cover (TCC)' and 'albedo (al)'. The TCC values are sums of high cloud cover (HCC), medium cloud cover (MCC) and low cloud cover (LCC). All of the data files of the Earth's total cloud coverage and its albedo contain values for each spatial grid point with a resolution of 3x3. When we use re-forecasts and re-analyses for comparisons with MODIS data, we must calculate one mean value for each the forecast days in a way that is starts at the same UTC as MODIS. All MODIS data are global mean values that begins at 12UTC meanwhile all re-analyses are 'snapshots' of the atmosphere at 00UTC. This time shift is taken into account in further data processing, the mean value at 12UTC is extracted from the re-analyses due to the assumption that there is a linearly change between the current and the next day. The daily averages of the forecasts are determined by weighting forecasts starting at 12UTC (in the middle of the day) with 50% and each of the 00UTC (from previous and next day) measurements with 25%, this procedure extracts daily averages beginning at 12UTC in each forecast day. We get a forecast lead time of six days which is ready to be used in further data analyses. Any possible biases in the re-analyses and forecasts are subtracted from the calculations. In addition to the data files, global mean values are retrieved from all data files to make the statistics less demanding and the program running-time fast. In this way, we avoid going repeating the steps described in section 4.1 for Monte-Carlo Bootstrap-based statistics ~16,000 times which requires more computational power.

4. Method

This study is relying largely on Monte Carlo methods which become handy in problems where there is a lack of data and one of the parameters of consideration isn't occurring in regular time intervals. Statistics is a powerful tool in our case where we deal with a space-weather phenomenon, a FD, and atmospheric variables. FDs are detected by multiple neutron monitors located in different places on Earth. The monitors count the number of neutrons produced by the secondary particle shower in the upper atmosphere. Changes in GCRs is detected by integrating the particle scatter for the whole planet by the use of multiple monitors. The FD values are adopted from table 1 in [9] and these values are ranked according to percentage strength of ionization. Datasets of the atmospheric variables are time series of global mean values. Cloud coverage data are retrieved both from ERA-I and MODIS which is also used by Svensmark [9].

4.1 Monte-Carlo Bootstrap-based statistics

The Monte Carlo bootstrap method is developed to rank the impact of FDs on ionization of the lower atmosphere. The method compares with a large number N_B of randomly selected days with all FD-event days, this comparison can tell how significant are the effects of the FDs. The aim of this method is to check how many measurements are left when we only count the signal of FD days that are less than the signal of randomly selected days drawn from the bootstrap sample - from here comes the name '*bootstrap*'. In this study we operate with thirteen different FDs between years 2000-2007. For each of these FDs we create a time series for our atmospheric variables of 36 days which goes from day -15 and day 20 after a specific FD event happening at day 0. The reason of choosing 36 days is that we avoid artificial or long-term changes in the atmospheric variables due to instrumentation. Any linear trend is removed in the time series of consideration to retrieve a non-biased response from the FD. The collection of FD units is then denoted $F_i(t)$. The same is done for the N_B random days so this is here the first steps of the bootstrapping part are made. The effect (or say signal) of FD is largest between the days t_1 and t_2 inside of the time series of 36 days. Within this range the randomly generated FD days are compared with the 'actual' FD days. This comparison is called Achieved Significance Level (ASL). All of the aforementioned steps will be follow-up in terms of equations in the following parts. The first equation we write in our numerical statistical model is a weighted sum of the number of FDs, N_{FD}, in our sample

$$FW(t) = \sum_{i=1}^{N_{FD}} F_i(t) w_i \tag{4.1}$$

Where w_i is a statistical weight that satisfies $\sum_{i=1}^{N_{FD}} w_i = 1$. We looked at 13 FDs and therefore made a sum with $N_{FD} = 13$. For comparisons, three different weight distributions are used. The first weight distribution is determined by using the strength of the individual FD

$$w_i = \frac{FD_i(\text{strength})}{\sum_{j=1}^{N_{FD}} FD_j(\text{strength})} \tag{4.2}$$

The other proposed distributions are retrieved by either defining equal weights to all FDs or giving only the five strongest FD a weight while setting the weights of the other FDs to zero. The other two weight distributions are

$$w_i = \frac{1}{N_{FD}} \quad \text{for } i = [1,2, \dots N_{FD}] \tag{4.3}$$

$$w_i = \begin{cases} 1/5 & \text{for } i = [1,2, \dots 5] \\ 0 & \text{for } i = [6,7, \dots N_{FD}] \end{cases} \tag{4.4}$$

Hereafter, we can determine the response or signal of the FD, denoted as FS, in the time series of consideration, after deciding which weight distribution we'll use.

$$FS = \sum_{t=t_1}^{t_2} FW(t) \tag{4.5}$$

The response is a scalar which is measured by integrating the weighted sum from day t_1 to t_2. The choice of day $t_1$and t_2 depends on the individual time series of $FW(t)$, t_1 is the first day where

$$BW_j = \sum_{i=1}^{N_{FD}} B_{i,j}(t) w_i \tag{4.6}$$

the parameter shows are remarkable change and begins to decline and t_2 is the final day of that response. The variable start getting back to normal state after t_2.The bootstrapping comes into use after going through the aforementioned steps. Bootstrap statistics is in general excellent in situations where the underlying statistical distributions are unknown and in situations where there might be issues such as autocorrelations inherent to the time series. To retrieve a bootstrap sample of our dataset we go through all of the same steps as before but this time the FD samples are generated randomly so that it picks out a random onset date of FD from the Table 1. Each of the bootstrap samples contains N_{FD} sample units. The final number of bootstrap samples is N_B - a very large number which can probably be $\geq 10^4$. As before we can apply weights (same weights as before since we have N_{FD} sample units) to measure the weighted sum of the *j*'th bootstrap sample unit, $B_{i,j}(t)$. Likewise, the response of the *j*'th bootstrap sample unit is given as

$$BS = \sum_{t=t_1}^{t_2} BW_j \tag{4.7}$$

A measure for the test statistics is denoted as $XFW(t)$ and it is given as

$$XFW(t) = FW(t) - \frac{1}{N_B} \sum_{j=1}^{N_B} BW_j \tag{4.8}$$

where look at the difference between the weighted time series of FD and the corresponding mean value of the bootstrap time series to see how close are these two quantities to one another. The corresponding integrated test signal or test response is

$$XFS = FS - \frac{1}{N_B} \sum_{j=1}^{N_B} BS_j \tag{4.9}$$

The distributions from the bootstrap sample and the integrated signal is defined as

$$DBW_j(t) = BW_j(t) - \frac{1}{N_B} \sum_{j=1}^{N_B} BW_j \tag{4.10}$$

$$DBS_j = BS_j - \frac{1}{N_B} \sum_{j=1}^{N_B} BS_j \tag{4.11}$$

Now we can determine whether the expected values, XFS and XFW, are drawn from the same distribution as the bootstrap sample. This can be done by measuring the probabilistic value known as an achieved significance level (ASL)

$$ASL_{boot}(t) = \{\text{Number of measurements } DBS_j \geq XFS\}/N_B \tag{4.12}$$

The modeled distribution of the integrated signal, *XFS*, or the test statistic, *XFW(t)*, can be compared with the empirically determined distribution functions achieved from the bootstrap sample, DBS_j or $DBW_j(t)$. The value for ASL is expected to be between 95-100% if there's a significant response from the FD. The smaller ASL, the stronger is the evidence of having no signal in the atmospheric parameter due to the Forbush decrease. ASL will be regarded as a proxy for eliminating the forcing from a FD.

Order	Date	Decrease (%)	Order	Date	Decrease (%)
1	31/10/2003	119	8	17/7/2005	47
2	19/1/2005	83	9	27/7/2004	45
3	13/9/2005	75	10	31/5/2003	44
4	16/7/2000	70	11	25/11/2001	39
5	12/4/2001	64	12	15/5/2005	38
6	10/11/2004	53	13	28/8/2001	37
7	26/9/2001	50			

Table 1 Adapted from [9]. An 'from strong to weak' ordered list of FD events in 2000-2007 measured by neutron monitors. The percentage decreases are the strengths of the different FDs. The weights used in further calculations are based on this table.

Order	Date	Decrease (%)	Order	Date	Decrease (%)
14	13/6/1991	87	20	27/8/1998	36
15	29/10/1991	56	21	10/5/1992	35
16	9/7/1991	54	22	27/2/1992	33
17	25/3/1991	48	23	18/2/1999	33
18	25/9/1998	45	24	2/5/1998	28
19	10/9/1992	44			

Table 2 Adapted from [9]. Extended version of Table 1 with all DF events in 1990-2000. The list continues from the end of Table 1. NB the combinations of Table 1 and Table 2 together is not ranked due to strength but Table 2 is alone ranked due to strength in the period 1990-2000.

5. Results

In the first three figures (Fig. 1, 2 and 3) the integrated signal of various FDs is plotted. The weighted sum, *FS*, of thirteen FD-events shown on a world map extracts which geographical locations are affected the most. The hypothesis proposed by Svensmark in 1997 says that marine clouds are affected the most after a FD - and that there is a remarkable difference between clouds over seas and clouds over land [11].The

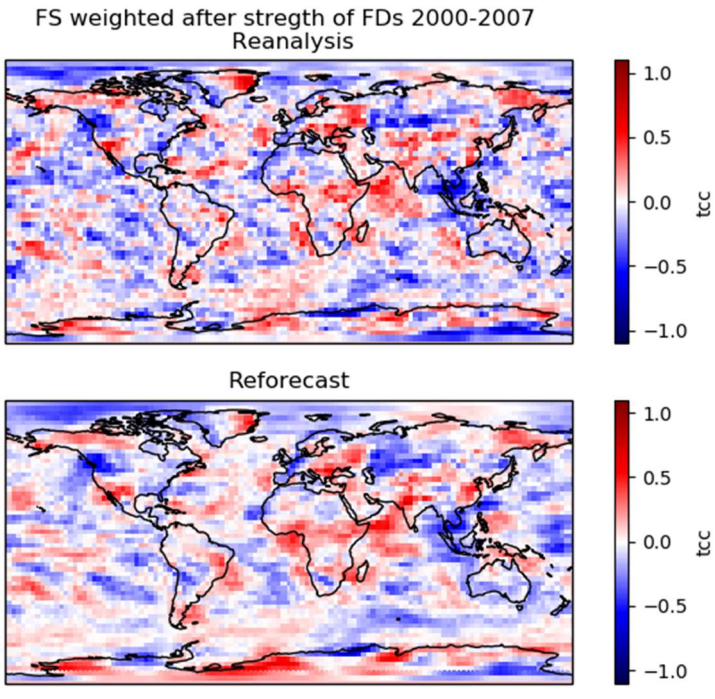

Figure 1 FS values integrated from $t_1 = 4$ to $t_2 = 10$ for the FD in 2000-2007 from Table 1. All FDs are weighted according to strength, which means we use Equation 4.2. The figure above shows the FS values for the re-analysis data for TCC and the figure below shows the corresponding re-forecasts for TCC. The global mean FS for the re-analysis is -0.02382 and -0.01194 for the re-forecast.

results we got from weather re-analyses and re-forecasts doesn't verify this trend. The cloud responses over oceans are showing both an increase and a decline of cloud cover. We have used all three different weightings. Fig. 1, 2 and 3 shows how the FS values are distributed when we switch from weighting the FDs by strength to weighting them equally and in the last figure, Figure 3, we only look at the five strongest FDs. Be aware of the different color scales in

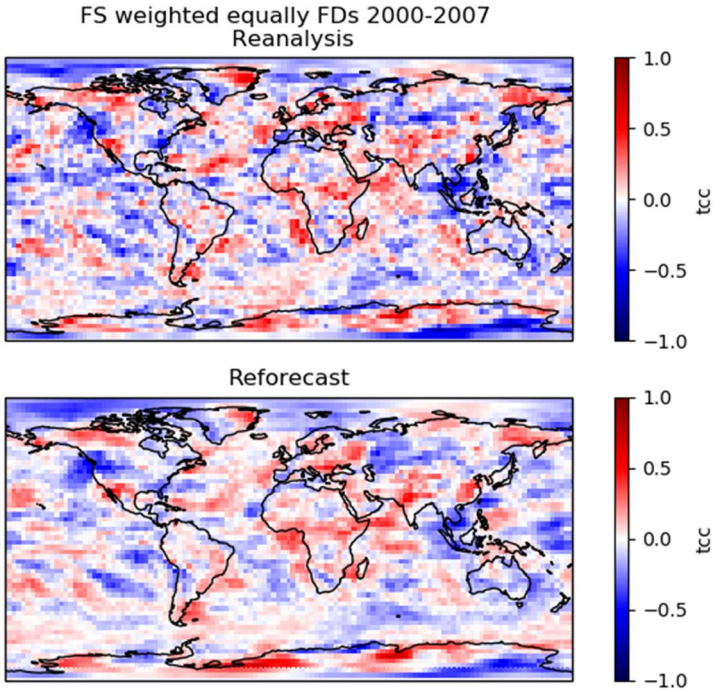

Figure 2 Again the plot shows FS integrated from $t_1 = 4$ to $t_2 = 10$ as in Fig. 1 but with weights that are equal (i.e. $w_i = \frac{1}{13}$) on all the FDs that undergoes the integration. The global mean FS for the re-analysis is -0.01972 and -0.01193 for the re-forecast.

each figure. Negative values (blue) represents a declines and positive values (red) represents increases. We are operating with two types of data one set which is already averaged over the whole globe and the other - which is used for the world plots only (Fig. 1-3). The calculated global averaged FS values for the re-analyses and re-forecasts shown in the world plots are written in the figure text boxes. The reforecasts that are weighted equally and the re-forecasts that are weighted by strength shows similar patterns over the same locations but the signals are stronger in the *'weighted by strength'* plots. In Fig. 3 the signals from the FDs

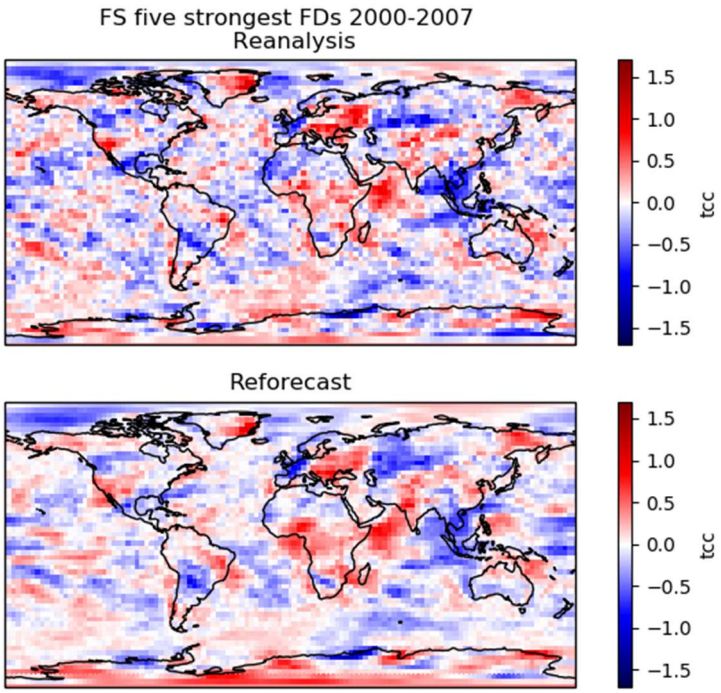

Figure 3 *FS* integrated from $t_1 = 4$ to $t_2 = 10$. The weights for the five strongest FD from Table are obtained from equation 4.4. The global mean FS for the re-analysis is -0.02820 and -0.00663 for the re-forecast.

are much larger compared to the shown in Fig. 1 and in Fig. 2. The color scale range for *the five strongest* plots are -1.7 to +1.7. Furthermore, the bootstrap method is applied on the globally averaged TCC data and CF data where the ASL values are determined. The globally averaged curves are made for two different time periods: 1) only FDs from 2000 to 2007 are analyzed, during this period MODIS CF data and ERA-I re-forecast and re-analysis TCC data are covered, and 2) we analyze the FDs from 1990-2007 which gives a total of 24 FDs. During the 1990-2007 period, ERA-I re-forecasts and re-analyses are available. The global averaged cloud cover variations are used in Fig. 4, Fig. 5 and Fig 6 which show the weighted sum of the FDs in Table 1, the summed signal, *FS*, is calculated from $t_1 = 4$ to $t_2 = 10$ after the onset of the FD. The Equation 4.5 in section 4.1 is used for calculating FS. Any linear trends are removed from

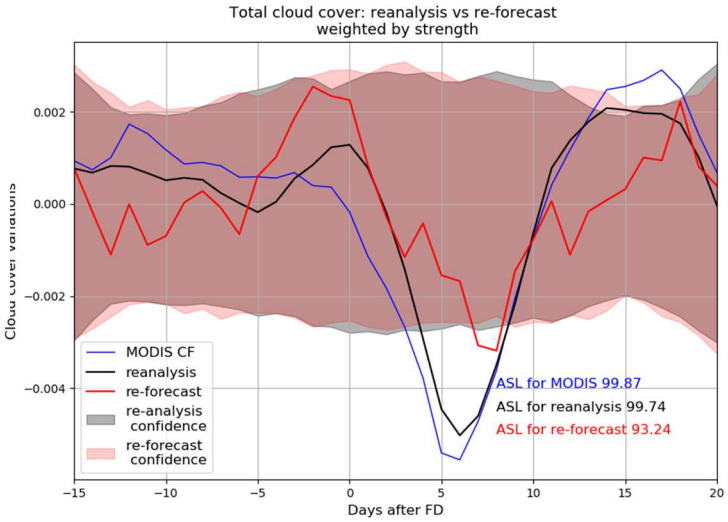

Figure 4 Average curves of six days are shown for the cloud cover variations in MODIS CF, ERA-I re-analysis TCC and ERA-I re-forecast TCC. The plot shows the weighted sum, FW, and the signal FS is measured from the 4th -10th day after the FD. The FS is -0.02266 for the re-analysis and -0.01136 for the re-forecast. The curves are the weighted by strengths in years 2000-2007 from Table 1. The ASL values are obtained by generating 10^4 bootstrap samples of our cloud data.

the 13 different time series. Fig 4, 5 and 6 are made using the same method but with different weights i.e. the weights from Eq. (4.2), (4.3) and (4.4). In Fig. 4 all FD-events are ranked by their strength. In Fig. 5, equal weights of $w = \frac{1}{13}$ are applied to all FDs. In Fig. 6 weights are applied equally on the five strongest FDs only. The ASL

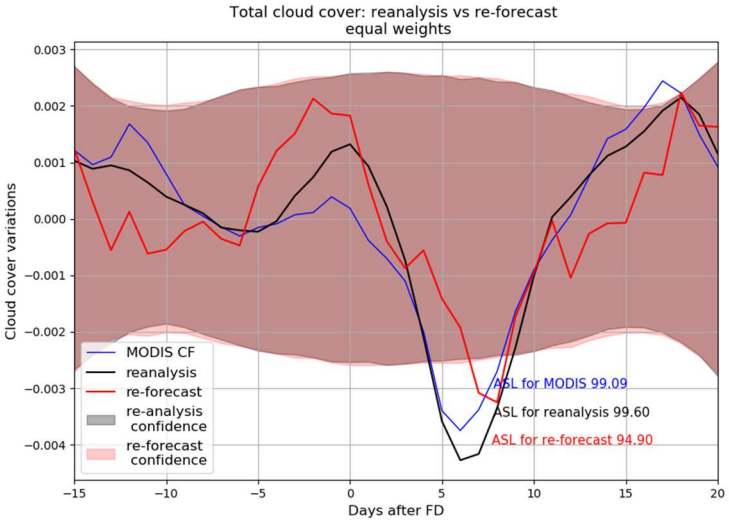

Figure 5 The exact same methpod as in Fig. 4 is applied here - except here we weighted all FDs between 2000-2007 equally i.e w = 1/13. The FS for the re-analysis is -0.01974 and -0.01196 for the re-forecast.

percentage for each of the three curves are measured by using Equation 4.12 - in these analyses we compared $N_B = 10^4$ bootstrap samples. Note the limit of the values in the y-axis is different in all three figures. The shaded red and grey curves in Fig. 4, 5 and 6 shows the 90% confidence intervals of the six days average re-forecasts and re-analyses. The 95th and 5th percentiles are retrieved from the bootstrap samples. The subtraction of linear trend determines the shape of the 'confidence curve'. Fig. 7 shows the weighted sum, FW,

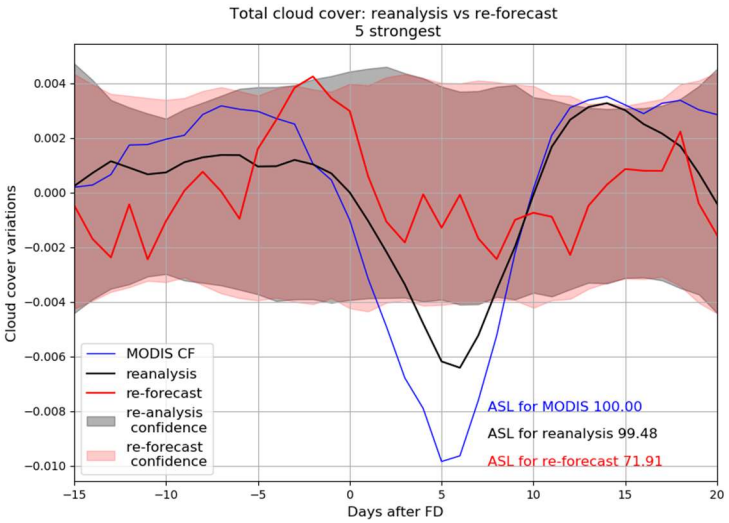

Figure 6 The exact same procedure as in Fig. 4-5 is repeated here - except here we only look at the five strongest FDs according to Table 1. Like in Figures 4-5, these curves shows the summed signal of FDs between day 4 and day 10 after the FD-event. Both MODIS and ERA-I re-analysis agree but the re-forecast shows different behavours due to different weight techniques. In this case the FS values for the re-analysis and for the re-forecast is -0.02815 and -0.00655.

when all three types of weights are applied on all of the FD events from Table 1 and Table 2. All FS values are written in figure textbox for Fig. 7. According to the results shown in Fig.

7, the middle figure that shows the weighted sum by strength is perhaps the most realistic representation of the response of the cloud to an FD event. The FS values for this plot is: -0.00521 for the forecast and -0.01093 for the analysis. The signal in the re-forecast is approximate as half as strong as the signal in the re-analysis (be aware of a small ALS in the re-forecast). The accuracy of the TCC re-forecast has been advanced with approx. 8% in the years 1990-2007. The accuracy changes are checked by calculating the percent error of the re-forecast where the verifying re-analysis is set as the true value.

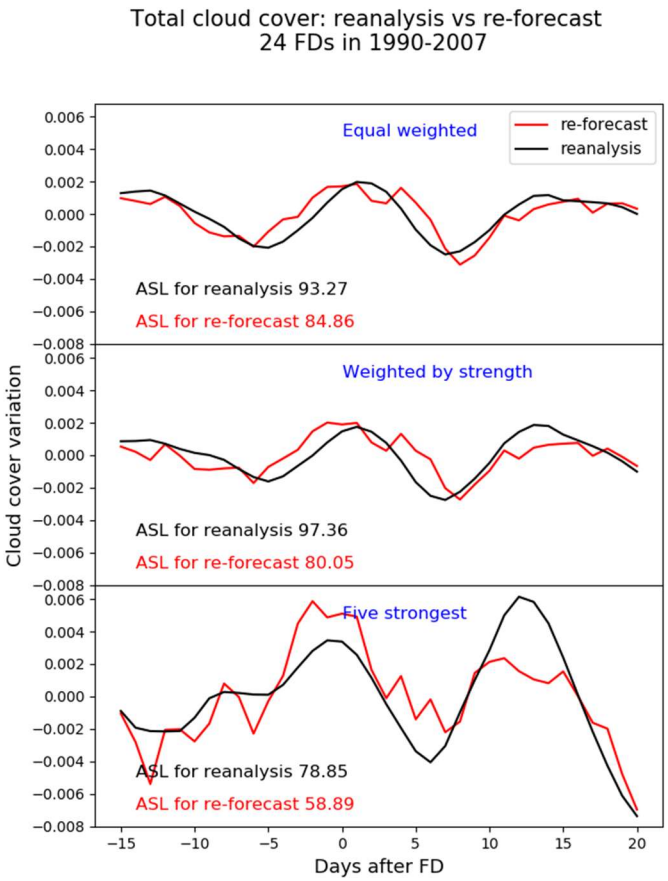

Figure 7 shows the three different weighted sums, *FW(t)*, of the 24 FDs in 1990-2007 from both Table 1 and Table 2. On the top is shown the equal weighted sum, in the middle the weighted by strength and at bottom is the sum of the five strongest FDs in 1990-2007. The five strongest in this case is the top 4 FDs from Table 1 and the first FD from Table 2. The two uppermost subplots, *equal weighted* and *weighted by strength*, are both in agreement, and the re-forecasts follows closely the re-analysis. The ASL values are no longer as high as in the previous calculations where only 13 FD event were included in the analysis. The FS values which are integrated from day 4 to 10 is, starting from top subfigure: -0.00587 for the forecast and -0.00908 for the analysis (equal weighted), -0.00521 for the forecast and -0.01093 for the analysis (weighted by strength) and -0.00263 for the forecast and -0.01236 for the analysis (for the five strongest).

6. Discussion and Conclusions

Nye proposed in 1959 that ions produced by GCRs in the lower atmosphere are the one variable that varies the most due to solar variability/cycle [11]. The long-term connection between CR and climate, hence clouds, has been tested in ice core archives. J. Beer made correlations between the combined flux of 10Be + 36Cl with δ18O data and CH4-data to test the cloud-climate theory. None of these parameters are correlated during the period 36-41.5 ka B.P during the Laschamp event (see Fig. 7). Most litterature is critical concerning the long-term links. The short-term change in the entering CR due to FD event are of same order as the solar variability but on a different

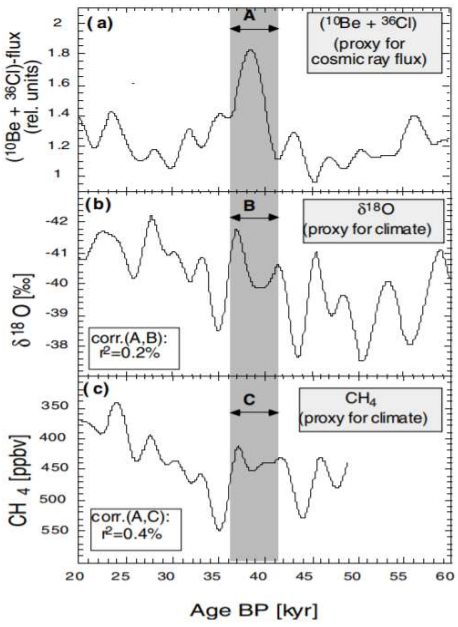

Figure 8 Comparison of the combined 10Be-36Cl flux with the climate parameters δ18O and CH4. The shaded area is 36-41.5 ka B.P, the Laschamp event occurred ~41ka (Beer, Figure 5: ICE CORE DATA ON CLIMATE AND COSMIC RAY CHANGES, 2001).

time scale. Assuming there is a link between CR and clouds, the signal will stay for a couple days. We have for the first time, after the evolvement of more accurate weather prediction models, used weather forecasts to either confirm or reject the link between cloudiness and FD by using a bootstrap analysis method. We looked at the periods 2000-2007 and 1990-2007 separately. There have not been any FDs after 2005 because the Sun is currently in the least active cycle in 30 years. Even though ERA-I is continually getting updated there is no opportunity to look at FDs until recently. The sun was very active in the year 2005 which resulted in no less than four FD events during that year, and the same applies for the years 2001 and 1991. These years (1991, 2001 and 2005) are dominating the results. High ASL-values, >99.00%, are obtained in the short-term signal of FD in the following days in the time period 2000-2007. The MODIS CF curves are exaggerating the signals and always giving high ASLs. The different weighting techniques gave different ASL values for the re-forecasts while the re-analyses are not showing remarkable differences in ASL due to weighting (in Fig. 4-6 for time period 2000-2007). However, the purpose of showing the curves in Fig. 4-6 together with the confidence shades is to show how likely or unlikely an FD-event is. In Fig. 4, all three curves show a decline in cloud cover variation, FW, which is below the lower percentile. Both MODIS CF and the re-analysis TCC have ASL values close to 100% and the ASL for the forecast is likewise very close with a value of 93.24%. These 94.90% tells us that only in 6.76% of the samples will have weaker signal than the one drawn from the FS - which implies that these curves are not random. The real concern is in fact that the shape of the curve changes a lot when we go from weighting equally or by strength to only putting weights on the five strongest FDs. While the re-forecasts drawn in Fig. 4 and Fig. 5 are roughly in agreement according to their shapes and the times at which they decline meanwhile the forecast in Fig. 6 tells another story. The ASL for the signal in the of five strongest FDs in the re-forecasts has been computed multiple times and it appears to vary around 70%. The *FW* for the re-forecasts with the weights from Eq. (4.4) are not showing as significant behavior as in the other cases where the weights from Eq. (4.2) or Eq. (4.3) were applied. Eq. (4.4) is poor weighting method for both the analyses made for 2000-2007 and 1990-2007. The physics of the measured changes in the re-analyses of TCC in Fig. 4, 5, 6 is discussed briefly in [9] (where the calculations are based on MODIS cloud variables). The peak to peak variations in the radiative budget during a solar cycle is 1-1.5 W/m^2 (Shaviv, 2008; Howard et al., 2015) and the variations due to an FD is a bit smaller than this. The absolute change in the low cloud fraction is ≈2% which corresponds to a relative change of ≈5% [9]. Changes of 1-2% in low cloudiness could have a significant effect on temperatures through changes in albedo (Palle and Butler (2002), [5]). The absolute change and relative change in the re-forecasts are smaller.

According to the calculated FS values, shown in Fig. 7, the signals achieved from the re-forecasts are weaker than the signals achieved from the verifying re-analysis but since the achieved significance levels are small these results cannot verify what is exactly happening to the re-forecast after the system experiences an FD. After including more FDs, we see - especially in the re-forecasts - how less significant the signals become. The equal-weighted plot and the plot that is weighted by strength are both showing that the re-forecasts follow the re-analysis closely.

The summed response in re-forecast TCC shows a tendency of getting less significant when less FDs are considered - the ASLs are higher when more FD's are included whether the re-forecasts

are weighted equally or according to strength. In Fig. 7, all ASL has declined but only FDs that are ranked due to strengths are showing significant results. The signals in the re-forecasts are somehow as half as strong as the signals in the re-analysis. Our first hypothesis was that the re-forecasts shouldn't show any signal and hence no change in the TCC - one can argue that the short-term impacts from FD can't be predicted in a numerical weather prediction. The alternative is if the results show both the re-analyses and re-forecasts are following each other closely then the signal may primarily be due to weather noise, artefacts and other internal sources. One reason for why the signals are exaggerated in the period 2000-2007 could be due to MODIS data meanwhile in the period 1990-2000 where MODIS wasn't in orbit the signal seems to become less significant, hence we get a less significant signal for the whole period namely 1990-2007. The graphs that are shown in Fig. 7 are all showing a 'small jumps' in the re-forecasts over day 2 to day 6 after the onset of FD. The jumps could be due to weather noise, artefacts and the accuracy of the ERA-I re-forecasts which has changed over time. The enhancement of re-forecasts is perhaps important to consider when one looks at a long time-span i.e. 1990 to 2007 where the accuracy has changed with about ~8%. This study cannot verify the CR-cloud cover link in both re-analysis and re-forecast TCC, different conclusions can be drawn for different FD-events. In general, we could eliminate artefacts in the data by changing our approach in the analysis. Instead of removing the linear trend over the 36-day time-series one could make low-pass by using Fourier transform to remove all slow evolving signals. However, it should not impact the final results so much but could make them more accurate. The real atmosphere is much complex and the weather varies a lot with seasonal changes. Perhaps the time span of 36 days is too long and could be shortened by ten days (by cutting off five days in the start and five days in the end). No significant signals were obtained in the re-forecasts in Fig. 6 and Fig. 7. The signals in the re-forecasts in Fig. 4 and Fig. 5 are with significance showing that the re-forecasts are closely following the re-analyses. One may conclude that FDs doesn't affect the short-term weather as first thought - otherwise it would have appeared in the re-forecasts as a great error. This study is largely in agreement with Laken (2012) who found that there is no robust evidence of a widespread link between the cosmic ray flux and clouds [7]. In literature, only few studies of the short-term CR-clouds link due to FD have obtained statistically significant result with satellite-based observations, Svensmark et. al (2009, 2012, 2016). Laken (2009) and Čalogović (2010) have made similar tests on FD events but failed to see any statistical signifance signals [7].

References

[1] Beer, J (2001). *Ice Core Data on Climate and Cosmic Ray Changes*. In J. Kirkby and S. Mele, editors, Proc. Workshop on Ion–Aerosol–Cloud interactions, CERN, 18–20 April 2001, CERN, CERN Yellow Report, CERN-2001-007 (ISSN 0007-8328, ISBN 92-9083-191-0), pages 3–11.

[2] Cane, Hilary. (2012). *Coronal Mass Ejections and Forbush Decreases*. Space Science Reviews. 93. 55-77. 10.1023/A:1026532125747.

[3] Chen, P. F. (2011), *Coronal Mass Ejections: Models and Their Observational Basis*, Living Rev. Sol. Phys. **8**, doi: https://doi.org/10.12942/lrsp-2011-1.

[4] Dunai, Tibor J. *Cosmogenic Nuclides: Principles, Concepts and Applications in the Earth Surface Sciences.* Cambridge University Press (2010).

[5] J.S. D'Aleo (2016)*, Chapter 15 - Solar Changes and the Climate,* Editor(s): Don J. Easterbrook, Evidence-Based Climate Science (2nd Ed.), Elsevier, Pages 263-282, ISBN 9780128045886, https://doi.org/10.1016/B978-0-12-804588-6.00015-X. (http://www.sciencedirect.com/science/article/pii/B978012804588600015X)

[6] Kalnay, E. (2003), *Atmospheric modeling, data assimilation and predictability*, Cambridge University Press, United Kingdom.

[7] Laken, Benjamin A. Enric Pallé, Jaša Čalogović, Eimear M. Dunne (2012). *A cosmic ray-climate link and cloud observations.* J. Space Weather Space Clim. 2 A18. DOI:10.1051/swsc/2012018

[8] Singh, A.K., Siingh, D., Singh, R.P. (2011), *Impact of galactic cosmic rays on Earth's atmosphere and human health*, Atmos. Environ., 45, pp. 3806-3818.

[9] Svensmark, J., M. B. Enghoff, N. Shaviv, and H. Svensmark (2016), *The response of clouds and aerosols to cosmic ray decreases*, J. Geophys. Res. Space Physics, 121, 8152–8181, doi:10.1002/2016JA022689.

[10] Svensmark, H., M.B. Enghoff, N.J. Shaviv & J. Svensmark (2017), *Increased ionization supports growth of aerosols into cloud condensation nuclei*, Nature Communications **8**, 2199, doi:10.1038/s41467-017-02082-2.

[11] Svensmark, H., and E. Friis-Christensen (1997), *Variation of cosmic ray flux and global cloud coverage—A missing link in solar-climate relationships*, J. Atmos. Sol. Terr. Phys., 59, 1225–1232, doi: 10.1016/S1364-6826(97)00001-1.

Appendix

Table 1. The 26 Strongest FD Events Over the 1987–2007 Period, Sorted by Strength[a]

Order	Date	Decrease (%)	A	$\pm\delta A$	γ
1	31/10/2003	119	229	10/9	-0.87 ± 0.02
2	13/6/1991	87	121	4/4	-0.74 ± 0.01
3	19/1/2005	83	273	16/15	-1.09 ± 0.02
4	13/9/2005	75	233	34/33	-1.07 ± 0.04
5	15/3/1989	70	93	14/12	-0.72 ± 0.06
6	16/7/2000	70	131	7/7	-0.86 ± 0.02
7	12/4/2001	64	153	12/11	-0.96 ± 0.03
8	29/10/1991	56	83	4/4	-0.76 ± 0.02
9	9/7/1991	54	84	4/4	-0.78 ± 0.02
10	29/11/1989	54	173	13/12	-1.08 ± 0.03
11	10/11/2004	53	95	8/8	-0.84 ± 0.04
12	26/9/2001	50	203	16/15	-1.18 ± 0.03
13	25/3/1991	48	82	15/13	-0.82 ± 0.07
14	17/7/2005	47	147	14/13	-1.07 ± 0.04
15	25/9/1998	45	123	45/33	-1.01 ± 0.14
16	27/7/2004	45	97	7/7	-0.91 ± 0.03
17	10/9/1992	44	206	46/38	-1.24 ± 0.09
18	31/5/2003	44	61	3/3	-0.74 ± 0.02
19	25/11/2001	39	75	15/13	-0.87 ± 0.08
20	15/5/2005	38	132	16/14	-1.12 ± 0.05
21	28/8/2001	37	152	15/14	-1.19 ± 0.04
22	27/8/1998	36	38	24/15	-0.63 ± 0.21
23	10/5/1992	35	50	6/5	-0.75 ± 0.05
24	27/2/1992	33	30	2/2	-0.57 ± 0.03
25	18/2/1999	33	38	3/3	-0.66 ± 0.03
26	2/5/1998	28	55	6/5	-0.88 ± 0.04

[a]The first and second columns are, respectively, the order and date of minimum cosmic ray flux. The third column shows the percentage decrease in ion production *relative* to the decrease in cosmic rays from solar maximum to solar minimum over a solar cycle. The final two columns display the parameters A and γ as obtained by the power law fit and defined in equation (6). The decrease from solar maximum to solar minimum, as fitted using equation (6), gives $A_{SC} = 336 \pm 46$ and $\gamma_{SC} = -1.10 \pm 0.04$. It is shown as the black curve of Figure 3. The uncertainty in A is given as an upper uncertainty/lower uncertainty. For example, A for the first event is 229^{+10}_{-9}. Note that no strong FD has occurred after 2007. Date is formatted as day/month/year.

Table 1 The complete table adapted from [9] showing 25 FD events in 1987-2007.